Optimal design with multiple displacement constraints

Matteo Bruggi
Department of Civil and Environmental Engineering, Politecnico di Milano, Italy
Email: matteo.bruggi@polimi.it

Hussein Ismail
Department of Structural Mechanics, Budapest University of Technology and Economics, Hungary,
Department of Civil and Environmental Engineering, Politecnico di Milano, Italy
Email: hussein.ismail@emk.bme.hu, hussein.ismail@polimi.it

János Lógó
Department of Structural Mechanics, Budapest University of Technology and Economics, Hungary
Email: logo.janos@emk.bme.hu

***Abstract*—A classical formulation used in the optimal design of elastic structures by distribution of isotropic material adopts the compliance, i.e. twice the strain energy, as the objective function, whereas volume plays the role of a constraint. It may be shown that, considering one load case only, this formulation is equivalent to a displacement-constrained volume minimization. When multiple load cases are addressed, the volume-constrained minimum compliance formulation is usually extended by considering as the objective function a weighted sum of the compliance values referring to each load case. This allows achieving structures that can sustain the forces belonging to any combination of the single load cases, with the main advantage that a volume constraint is the only enforcement to be processed in the optimization. Unfortunately, this formulation does not allow for a local control of the displacement field due the single load cases, as conversely required by technical codes used in structural design. Recent contributions in the field of stress-constrained topology optimization have shown that a very large number of local enforcements can be efficiently tackled by combining sequential convex programming and the augmented Lagrangian method. In this work, this numerical approach is implemented to solve minimum volume problems with multiple displacement constraints. The proposed approach can be used to design optimal structures in case of distributed loads or multiple load cases, with a full control of the displacement field, no matter how many nodes or load cases are considered. Applications are shown to discuss mechanical features of the achieved optimal layouts as well as parameters employed in the implemented numerical approach.**

I. Introduction

Topology optimization allows customizing structural components by distributing a limited amount of material within a given design domain in order to match prescribed gaols and constraints [1]. Among the others, the design operated by distribution of isotropic material is widely adopted by academia and industry to sketch lightweight structures, see [2]. Assuming as unknown the density field that governs the elastic modulus of the material, an optimization problem can be formulated to minimize the work of external loads at equilibrium (the so-called structural compliance), with constraints on the allowed amount of material (the available volume fraction). Since the compliance reads twice the strain energy, the problem is in turn equivalent to finding the distribution of the available amount of material such that the overall strain energy is minimized, i.e. the stiffness is maximized. Minimum compliance problems may be solved very efficiently, see in particular in [3].

The design of two dimensional structural elements is herein formulated as a displacement-constrained minimum volume problem under multiple load cases, see [4]. A displacement-constrained formulation allows investigating optimal layouts by enforcing requirements at the serviceability limit state. Maximum displacements are those prescribed e.g. by technical codes. The amount of material needed to meet the constraints is an outcome of the problem. This is used to perform comparisons when different loads/limits are considered for the same structural element.

When the controlled displacement is that at the loaded point along the direction of the applied force, the work of the external load at equilibrium is straightforwardly given by the scalar product of the controlled displacement and the applied force. Hence, the proposed problem is a compliance-constrained minimum volume problem, which is in turn equivalent to a classical volume-constrained minimum compliance problem. Indeed, the same solution (up to a scaling) is expected to arise when considering either problem, see [5].

When multiple load cases or distributed loads are dealt with, the enforcement of a set of displacement constraints is required. Recent contributions in the area of stress-constrained topology optimization have shown that large sets of local enforcements can be efficiently tackled by combining sequential convex programming and Augmented Lagrangian (AL) approaches without resorting to aggregation methods [1]. Within the family of sequential programming approaches, the Method of Moving Asymptotes (MMA) [6] is especially tailored for structural optimization since it may linearize objective function and constraints not only in the direct variables but also in the reciprocal ones, see also the application in [7]. In [8] an augmented Lagrangian approach is implemented where the original penalization term, see [9], is normalized with respect to the number of constraints.

In this work, this numerical approach is implemented to solve minimum volume problems with multiple displacement constraints. The proposed method can be used to design

978-1-6654-2495-0/21/$31.00 ©2021 IEEE

optimal structures in case of or multiple load cases including distributed loads, with a full control of the displacement field, no matter how many local constraints are dealt with. Preliminary numerical applications are shown to discuss mechanical features of the achieved optimal shapes. Parameters used in the simulation are presented, as well.

II. Design of the topology for minimum volume under displacement constraints

A. Formulation

A finite element discretization of a given design domain is operated, employing standard four-node displacement-based elements. A set of element-wise discrete design variables is considered. In the e-th of the n elements of the mesh, $0 < \rho_e \leq 1$ is a variable that controls the "density" of material, according to the Solid Isotropic Material with Penalization (SIMP) [10]. In the e-th element, the constitutive matrix $\boldsymbol{C}(\rho_e)$ may be written as:

$$\boldsymbol{C}(\rho_e) = \rho_e^p \ \boldsymbol{C}_0, \tag{1}$$

where $\boldsymbol{C}_0$ is the inverse of the matrix for the material at full density, and p is an interpolation parameter that penalizes intermediate densities. In the numerical simulations, p is increased from 3 to 6 during the optimization, see the continuation approach implemented in [3].

A problem for the design of a displacement-constrained topology of minimum weight can be stated as:

$$\begin{cases} \min\limits_{0<\rho_e\leq 1} \mathcal{W} = \sum\limits_{e=1}^{n} \rho_e \, W_{0,e} & \text{(2a)} \\ \text{s.t.} \ \ \mathbf{K}(\boldsymbol{\rho}) \, \mathbf{U}_j = \mathbf{F}_j, \quad \text{for} \ \ j = 1...l, & \text{(2b)} \\ u_i \leq u_{lim,i}, \quad \text{for} \ \ i = 1...m. & \text{(2c)} \end{cases}$$

In the above statement, the objective function is the volume of the structural element, which is computed through the sum of the element contributions $\rho_e \, W_{0,e}$, being $W_{0,e}$ the volume of the e-th element for $\rho_e = 1$.

Eqn.(2b) prescribes the discrete equilibrium of the structural element. The global stiffness matrix $\mathbf{K}(\boldsymbol{\rho})$ is computed by assembling the element contributions that account for the constitutive law given in Eqn.(1). The element stiffness matrix can be conveniently written as $\rho_e^p \, \mathbf{K}_{0,e}$, where $\mathbf{K}_{0,e}$ refers to $\rho_e = 1$. For the j–th of the l load cases, $\mathbf{F}_j$ is the load vector, whereas $\mathbf{U}_j$ is the relevant nodal displacement vector.

The i–th of the m displacement components to be controlled is denoted by u_i. Eqn.(2c) enforces a prescribed limit $u_{lim,i}$, where $u_{lim,i}$ stands for the maximum displacement allowed at the serviceability limit state. Assuming that u_i is an entry of $\mathbf{U}_j$, i.e. that the i–th constraint refers to the j-th load case, one has:

$$u_i = \mathbf{L}_i^T \mathbf{U}_j, \tag{3}$$

where $\mathbf{L}_i$ is a vector made of zeros except for the entry referring to the i–th displacement degree of freedom, which takes unitary value.

B. Numerical implementation

Details are given in the following sections on the treatment of the density field to avoid well-known numerical instabilities while achieving crisp black/white layouts, and on the adopted gradient–based solution approach to the considered multi-constrained formulation.

1) Filtering: A linear filter [11], [12] is implemented on the element variables ρ_e to avoid potential issues that are well-known in topology optimization, i.e. the arising of mesh dependence and checkerboard patterns. The original variables ρ_e are mapped to the new set of $\tilde{\rho}_e$ as follows:

$$\tilde{\rho}_e = \frac{1}{\sum_n H_{es}} \sum_n H_{es} \, \rho_s, \tag{4a}$$

$$H_{es} = \max(0, r_{min} - \text{dist}(e, s)), \tag{4b}$$

where $\text{dist}(e, s)$ is the distance between the centroid of the e-th and s-th element, and r_{min} is the filter radius. Hence, the filtered densities are mapped to the set of projected (physical) densities $\widehat{\rho}_e$ in order to achieve crisp black/white solutions, see in particular the formulation proposed in [13]:

$$\widehat{\rho}_e = \frac{\tanh(\beta\eta) + \tanh(\beta(\tilde{\rho}_e - \eta))}{\tanh(\beta\eta) + \tanh(\beta(1 - \eta)}, \tag{5}$$

with $\eta = [0, 1]$ and $\beta = [1, \infty]$. In the numerical section $\eta = 0.5$, whereas β is smoothly increased during the simulations from 2 to 16, by adopting the continuation approach in [3]; solutions are given in terms of maps of $\widehat{\rho}_e$.

2) Solving algorithm: The optimization problem in Eqn. (2) is solved via mathematical programming, adopting the Method of Moving Asymptotes (MMA) [6] as minimizer. Displacement constraints are treated following the Augmented Lagrangian method implemented in [8].

At the k-th AL step, an unconstrained problem is considered whose objective function reads:

$$\mathcal{W} + \frac{1}{m} \sum_{i=1}^{m} \left(a_i^{(k)} \frac{u_i}{u_{lim,i}} + \frac{b^{(k)}}{2} \left(\frac{u_i}{u_{lim,i}} \right)^2 \right), \tag{6}$$

where $a_i^{(k)}$ is the i-th entry of the vector $\mathbf{a}^{(k)}$ of the lagrangian multiplier estimators and $b^{(k)} > 0$ is a penalty factor. MMA is used to find an approximate solution of the normalized function in Eqn.(6), which is in turn adopted to update the current values of the lagrangian multiplier estimators and penalty factor for the $(k+1)$-th step. In the numerical simulations, the number of MMA iterations per AL step has been set to 5. The overall process is repeated until convergence is achieved, i.e. the maximum difference in terms of the minimization unknowns in $\mathbf{x}$ between two subsequent step is less than 10^{-3}.

The adjoint method is used to compute sensitivity to run the gradient-based minimizer, see e.g. [1]. Accordingly, u_i in Eqn. (3) does not change when adding at the right hand side a zero function derived from the equilibrium of Eqn.(2b), i.e.:

$$-\boldsymbol{\lambda}_i^T \left(\mathbf{K}(\boldsymbol{\rho}) \mathbf{U}_j - \mathbf{F}_j \right), \tag{7}$$

where $\boldsymbol{\lambda}_i$ is any arbitrary but fixed vector. Hence, the derivative of u_i with respect to the h-th element unknown ρ_h may be

computed as:

$$\frac{\partial u_i}{\partial \rho_h} = \boldsymbol{L}_i^T \frac{\partial \mathbf{U}_j}{\partial \rho_h} - \boldsymbol{\lambda}_i^T \frac{\partial \mathbf{K}(\boldsymbol{\rho})}{\partial \rho_h} \mathbf{U}_j - \boldsymbol{\lambda}_i^T \mathbf{K}(\boldsymbol{\rho}) \frac{\partial \mathbf{U}_j}{\partial \rho_h}. \quad (8)$$

After re-arrangement of terms, one has:

$$\frac{\partial u_i}{\partial \rho_h} = \left(\boldsymbol{L}_i^T - \boldsymbol{\lambda}_i^T \mathbf{K}(\boldsymbol{\rho}) \right) \frac{\partial \mathbf{U}_j}{\partial \rho_h} - \boldsymbol{\lambda}_i^T \frac{\partial \mathbf{K}(\boldsymbol{\rho})}{\partial \rho_h} \mathbf{U}_j, \quad (9)$$

that can be in turn written as:

$$\frac{\partial u_i}{\partial \rho_h} = -\boldsymbol{\lambda}_i^T \frac{\partial \mathbf{K}(\boldsymbol{\rho})}{\partial \rho_h} \mathbf{U}_j, \quad (10)$$

where $\boldsymbol{\lambda}_i$ satisfies the adjoint equation:

$$\mathbf{K}(\boldsymbol{\rho}) \boldsymbol{\lambda}_i = \left(\frac{\partial u_i}{\partial \mathbf{U}_j} \right)^T = \mathbf{L}_i. \quad (11)$$

Eqn. (10) can be evaluated recalling that the derivative of the e-th element stiffness matrix with respect to ρ_h is equal to $p \rho_e^{p-1} \mathbf{K}_{0,e}$, being $\mathbf{K}_{0,e}$ the element stiffness matrix at full density. This sensitivity is null if $e \neq h$.

The derivatives with respect to the filtered variables $\tilde{\rho}_e$ and the physical ones $\widehat{\rho}_e$ can be easily evaluated by applying the chain rule to Eqn. (4) and Eqn. (5), respectively. It is also remarked that, at each iteration in the process, only one matrix inverse must be computed to evaluate constraints and their sensitivities. Indeed the linear systems in Eqn. (2b) and Eqn. (11) share the same coefficient matrix.

III. Numerical simulations

Preliminary numerical simulations are presented in this section. The $3L \times L$ cantilever in Figure 1 is considered adopting a mesh of 300×100 square finite elements. The filter radius r_{min} is 8.75 times the length of the element side. Unitary point forces, as well as a distributed load with unitary resultant, are considered in the optimization.

A. Point forces in single load case

At first, numerical simulations are shown to investigate the numerical method presented in Section II when addressing one force only (in a single load case).

Optimal layouts are sought considering the force P only, see Figure 1(a), and enforcing that the vertical displacement read at the loaded point is less than 1.25, 1.50, 1.75 times the value u_0 found in case of a cantilever made of full material. The achieved results are given in Figure 2, 3 and 4, respectively. All the solutions consist in black and white distributions of material. In all the cases the displacement at the loaded point equals the enforced bound u_{lim}, whereas the volume fraction reads 62.06%, 49.04% and 40.82%, respectively.

In view of the adoption of multiple load cases, an additional simulation is performed considering load Q, enforcing a maximum deflection at the loaded point equal to 1.50 times the value found in case of a cantilever made of full material, see Figure 1(b). The achieved solution is represented in Figure 5. The relevant volume fraction reads 50.38%.

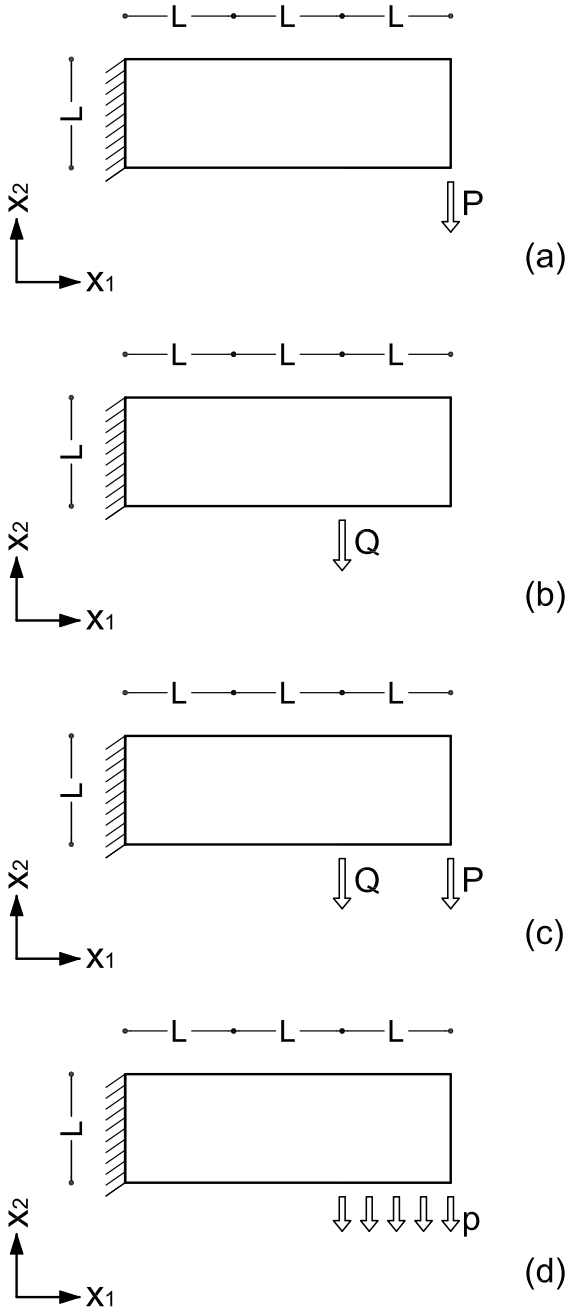

Fig. 1: Geometry and boundary conditions for the considered examples.

B. Multiple load cases

The formulation presented in Section II allows considering multiple load cases, controlling the displacements point-wise in each of them. Figure 6 shows the optimal cantilever found when load P and Q act independently, see Figure 1(c). Indeed, two load cases are defined to enforce in each of two that the vertical displacement under the loaded point is not above 1.5 times that read for a specimen made of full material. With a

Fig. 2: Optimal design considering the load P, with $u_{lim} = 1.25\,u_0$. Final volume fraction 62.06%.

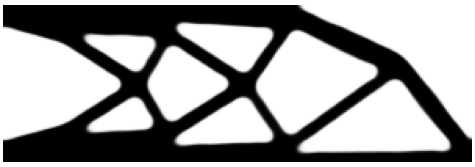

Fig. 4: Optimal design considering the load P, with $u_{lim} = 1.75\,u_0$. Final volume fraction 40.82%.

Fig. 3: Optimal design considering the load P, with $u_{lim} = 1.50\,u_0$. Final volume fraction 49.04%.

Fig. 5: Optimal design considering the load Q, with $u_{lim} = 1.50\,u_0$. Final volume fraction 50.38%.

slight increase in terms of volume fraction, now 51.42%, with respect to the layouts represented in Figure 3 (49.04%) and 5 (50.38%), a new design is found that fulfills the required performance in terms of structural response.

C. Distributed load

A final investigation is performed looking at the optimal design when a uniformly distributed load p acts along the bottom edge over a length equal to $L/3$ in the vicinity of the free end, see Figure 1(d). The multi-constrained formulation in Eqn.(2) allows enforcing local constraints at each one of the points at which the distributed load is applied, herein $m = 101$, all referring to the same load case. Again, it is required that each displacement is not bigger than 1.5 times that read for a specimen made of full material. The optimal solution is shown in Figure 7. A different design is found with respect to the previous ones. Indeed, the load application length and the new line of action of the resultant call for a new geometry. It is remarked that the solution is not far from the others, as far as the volume fraction at convergence is concerned (herein it reads 53.43%).

IV. Conclusion

In this contribution, a displacement-constrained minimum weight problem of topology optimization has been formulated to design lightweight structures that fully respect local enforcements on the deflection. An Augmented Lagrangian approach that has been recently proposed in the literature for the solution of stress-constrained problems attacked by sequential convex programming, has been herein implemented considering different types of displacement-constrained problems.

At first, the approach has been tested considering single load cases encompassing one point force. Then, it has been preliminary adopted to cope with multiple load cases including point forces, and to address a distributed load within a single load case. The adoption of filtering techniques originally proposed to achieve black and white design in compliance-based topology optimization is shown to give crisp results.

The ongoing research is focused on further tests of the method, especially considering problems with extended set of constraints, addressing multi-scale modeling as well, see e.g. [14].

References

[1] M.P. Bendsøe, O. Sigmund, Topology Optimization: Theory, Methods and Applications. Berlin: Springer, 2003.

[2] J. Lógó, H. Ismail, “Milestones in the 150-year history of topology optimization: A review”, Comput. Assist. Methods Eng. Sci., vol. 27(2-3), pp. 97-132, 2020.

[3] F. Ferrari, O. Sigmund, “A new generation 99 line Matlab code for compliance topology optimization and its extension to 3D”, Struct. Multidiscip. Optim., vol. 62, pp. 2211-2228, 2020.

[4] J. Lógó, B. Balogh, E. Pintér, “Topology optimization considering multiple loading”, Comput. Struct., .vol 207, pp. 233-244, 2018.

[5] W. Achtziger, “Topology Optimization of Discrete Structures”, in Topology Optimization in Structural Mechanics, Rozvany G.I.N. Ed., International Centre for Mechanical Sciences (Courses and Lectures), vol 374. Vienna: Springer, 1997.

[6] K. Svanberg, “Method of moving asymptotes - A new method for structural optimization”, Int. J. Numer. Methods Eng., vol. 24(2), pp. 359-373, 1987.

[7] M. Bruggi, “A constrained force density method for the funicular analysis and design of arches, domes and vaults”, Int. J. Solids Struct., vol. 193-194, pp. 251-269, 2020.

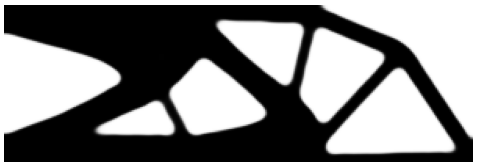

Fig. 6: Optimal design considering the load P and Q as two load cases, with $u_{lim,i} = 1.50\, u_{0,i}$ for $i = 1, 2$. Final volume fraction 51.42%.

Fig. 7: Optimal design considering the load p, with $u_{lim,i} = 1.50\, u_{0,i}\ \forall i$. Final volume fraction 53.43%.

[8] O. Giraldo-Londoño, G.H. Paulino, "PolyStress: A matlab implementation for local stress-constrained topology optimization using the augmented lagrangian method", Struct. Multidiscip. Optim., vol 63(4), pp. 2065-2097, 2021.

[9] D.P. Bertsekas, Nonlinear programming, 2nd edn. Nashua: Athena Scientific, 1999.

[10] M.P. Bendsøe, N. Kikuchi, "Generating optimal topologies in structural design using a homogenization method", Comput. Methods Appl. Mech. Eng. vol. 71(2), pp. 197-224, 1988.

[11] T. Borrvall, J. Petersson, "Topology optimization using regularized intermediate density control", Comput. Methods. Appl. Mech. Eng., vol. 190(37-38), pp. 4911-4928, 2001.

[12] B. Bourdin, "Filters in topology optimization", Int. J. Numer. Methods Eng., vol. 50(9), pp. 2143-2158, 2001.

[13] F. Wang, B. Lazarov, O. Sigmund, "On projection methods, convergence and robust formulations in topology optimization", Struct. Multidiscip. Optim., vol. 43(6), pp. 767-784, 2011.

[14] M. Bruggi, A. Taliercio, "Hierarchical infills for additive manufacturing through a multiscale approach", J. Optim. Theory Appl., vol. 187(3), pp. 654-682, 2020.